Enhancing cell migration in shape-memory alginate-collagen composite scaffolds: *in vitro* and *ex vivo* assessment for intervertebral disc repair

Olivier Guillaume[1,2], Syeda Masooma Naqvi[1,2], Kerri Lennon[1,2] and Conor Timothy Buckley[1,2]

[1] Trinity Centre for Bioengineering, Trinity Biomedical Sciences Institute, Trinity College Dublin, Ireland.

[2] Department of Mechanical Engineering, School of Engineering, Trinity College Dublin, Ireland.

*Corresponding author: Conor T. Buckley

E-mail address: conor.buckley@tcd.ie

Address: Trinity Centre for Bioengineering

Trinity Biomedical Sciences Institute

Trinity College Dublin

Ireland

Telephone: +353-1-896-2061

Fax: +353-1-679-5554

Key words: scaffold; alginate; collagen; migration; MSCs; shape-memory; intervertebral disc

Abstract

Lower lumbar disc disorders pose a significant problem in an ageing society with substantial socioeconomic consequences. Both inner tissue (nucleus pulposus, NP) and outer tissue (annulus fibrosus, AF) of the intervertebral disc (IVD) are affected by such debilitating disorders and can lead to disc herniation and lower back pain. In this study, we developed an alginate-collagen composite porous scaffold with shape-memory properties to fill defects occurring in AF tissue of degenerated IVDs, which has the potential to be administered using minimal invasive surgery. In the first part of this work we assessed how collagen incorporation on pre-formed alginate scaffolds influences the physical properties of the final composite scaffold. We also evaluated the ability of AF cells to attach, migrate and proliferate on the composite alginate-collagen scaffolds compared to control scaffolds (alginate only). *In vitro* experiments, performed in IVD-like microenvironmental conditions (low glucose and low oxygen concentrations), revealed that for alginate only scaffolds, AF cells agglomerated in clusters with limited infiltration and migration capacity. In comparison, for alginate-collagen scaffolds, AF cells readily attached and colonized constructs, while preserving their typical fibroblastic-like cell morphology with spreading behavior and intense cytoskeleton expression. In a second part of this study, we investigated the effects of alginate-collagen scaffold when seeded with bone marrow derived mesenchymal stem cells (MSCs). *In vitro*, we observed that alginate-collagen porous scaffolds supported cell proliferation and extracellular matrix (ECM) deposition (collagen type I); which secretion was amplified by the local release of TGF-ß3. In addition, when cultured in *ex vivo* organ defect model, alginate-collagen scaffolds maintained viability of transplanted MSCs for up to 5 weeks. Taken together, these findings illustrate the advantages of incorporating collagen as a means to enhance cell migration and proliferation in porous scaffolds which could be used to augment tissue repair strategies.

1. Introduction

Intervertebral disc (IVD) degeneration is known to be the predominant contributor to chronic low back pain (LBP). It is a major concern in an ageing society and has been reported to affect up to 5 million patients in the USA in 2011 [(1)] with estimated costs of $100 billion due to healthcare costs and lost productivity. [(2)] An estimated 85% of the adult population experiences LBP at least once during their lives. [(3)] Early stage treatments such as physical therapy and pain management with analgesics and anti-inflammatory drugs may provide pain relief, but offer no significant amelioration for acute stage degeneration. [(4)] For severe cases, disc herniation may be alleviated through surgical dissection of the bulging tissue (via discectomy), and complete disc removal followed by spinal fusion can be performed for advanced degenerated conditions. [(5)] However none of these available treatments aim to repair or regenerate the disc itself and not surprisingly surgical revisions are frequent. In this context, research into biomaterial and cell based approaches has intensified over the last decade to treat both nucleus pulposus (NP) and annulus fibrosus (AF) tissues. [(6-9)]

Recent attempts to close AF defects and promote tissue repair in an ovine model using partially degradable pre-formed composite implant made of polyglycolic acid and polyvinylidene have been reported. [(10)] These implants were capable of successfully retaining the NP within the central region of the IVD impeding disc herniation and also supported cell infiltration and matrix deposition after 12 weeks. However, evidence of AF tissue damage adjacent to the implantation site was observed and, as highlighted by the authors, such surgical procedures (biomaterials implantation plus suture placement) were extremely demanding for the surgeon. Limitations of employing pre-formed scaffolds include difficulties with drug incorporation and/or cell seeding issues as well as their inability to fill irregularly sized defects. [(11)] For this reason, extensive research involving injectable-

biomaterial candidates for NP regeneration have been explored, but surprisingly a limited number of similar systems have been targeted for annulus fibrosus tissue to date. [12-16] High-density injectable collagen gels have been investigated to fill punctured AF tissue in a rat tail model. Although no further sign of disc degeneration was observed in terms of hydration, as evaluated using MRI and disc height measurements post-implantation, incomplete AF tissue regeneration was observed in the inner region of the newly formed tissue, combined with a fibrous capsule in the outer part with dissimilarity in terms of extracellular matrix (ECM) composition compared to native AF tissue. [13]

In an attempt to fill AF defects and to promote tissue repair, we have previously reported the development of injectable porous scaffolds fabricated through the freeze drying of covalently crosslinked alginate based on carbodiimide chemistry. [16] Such scaffolds exhibit high pore interconnectivity and shape-memory properties ideal for this specific application, as it can expand and fill defects once hydrated. Although the shape-memory behavior of covalently crosslinked alginate is highly attractive, a disadvantage of this material is the lack of binding sites available for direct cell attachment. In an effort to increase the biocompatibility of these scaffolds we incorporated collagen onto covalently crosslinked porous alginate scaffolds. Advantages of using collagen as a biomaterial for tissue engineering are well documented. [17, 18] Collagen is highly biocompatible and is the most abundant organic material in the body. [19] Collagen has been successfully employed in hydrogel form or as cell culture substrates with several collagen-based matrices for tissue regeneration in commercial use. [20] However, collagen-based constructs are inherently mechanically weak and are susceptible to shrinkage as they cannot withstand the forces exerted due to cell contraction. [21, 22] To alleviate such limitations, we chose to combine collagen as a biological coating agent on covalently crosslinked alginate structure, which provides mechanical reinforcement.

The global objective of this study was to evaluate how incorporation of collagen in pre-formed alginate scaffold influences the physical properties of the shape-memory scaffolds and to assess its effect on AF cell migration and scaffold colonization *in vitro* and in an *ex-vivo* organ culture model. Finally, we explored the benefits of alginate-collagen scaffolds when seeded with bone marrow derived mesenchymal stem cells (MSCs) both *in vitro* and *ex-vivo* to assess (i) the survival of the MSCs post-implantation, and - (ii) if the presence of MSCs could promote resident AF cell recruitment into the implanted porous scaffold.

2. Materials and methods

2.1 Fabrication of injectable shape-memory scaffolds

2.1.1 Fabrication of alginate (Alg) scaffold

Porous alginate scaffolds were fabricated through a covalently crosslinking method using carbodiimide chemistry as previously described. [16] Sodium alginate (alginate Pronova UP LVG) was purchased from FMC Biopolymer (Novamatrix, Sandvika, Norway) and all other chemicals were obtained from Sigma-Aldrich (Arklow, Ireland). Briefly, alginate (final concentration 2%, w/v) was dissolved in morpholine ethanesulfonic (MES) acid buffer pH 6.0 and sterile solutions of N-hydroxysuccinimide (NHS) and 1-ethyl-3-(dimethylaminopropyl) carbodiimide (EDC) were added to the alginate solution at a final molar ratio of 2:1:2 for EDC : NHS : COO^-. Finally, the bifunctional crosslinker (adipic acid dihydrazide (AAD)), was added to the reactive solution at a concentration of 45 % (depending on n_{NH2} / n_{COOH}), rapidly homogenised and cast in a mould. The crosslinking reaction was allowed to proceed overnight followed by repeated washing in deionized water to remove any unreacted reagents. Porous scaffolds were obtained using a freeze-drying process (Labconco Triad™, Kansas City, MO USA), at a freezing temperature (T = -30ºC) to allow ice crystallization and finally sublimated under vacuum (0.2mBar) for 18 hrs at a temperature of -10°C to create the porous

network. After the freeze-drying process, scaffolds were created using a sterile biopsy punch (3 or 5 mm Ø x 3 mm H).

2.1.2 Fabrication of alginate–collagen (Alg-Coll) scaffolds

Collagen type I (extracted from rat tail, BD biosciences, Oxford, United-Kingdom) was incorporated into the pre-formed freeze-dried porous alginate scaffold during a rehydration step. Briefly, alginate scaffolds (Alg) were individually collapsed using a tweezers and rehydrated with sterile collagen solutions of different concentrations (0, 1.13, 2.26 and 4.52 mg/mL corresponding to the groups A, B, C and D respectively). The alginate – collagen scaffolds (Alg-Coll) were subsequently freeze-dried using the same protocol previously described [16] and subjected to dehydrothermal treatment (DHT, at 110°C during 24 hrs) in order to physically crosslink the collagen chains and stabilize the structure. This protocol was selected as it has been previously demonstrated to limit the denaturation of collagen chains in composite scaffolds. [23, 24]

2.2 Scaffold characterization

2.2.1 Determination of swelling ratio

In order to evaluate the influence of collagen incorporation on water uptake capacity and on shape-memory recovery behavior of the alginate-based scaffolds, the swelling ratio of groups A, B, C and D were determined as follows. Scaffolds (5 mm Ø x 3 mm H, n = 3) were collapsed with a tweezers for 30 sec., weighed (*W0*) and subsequently rehydrated with deionized (DI) water for 5 min., which was a sufficient period of time to allow scaffolds to fully swell. Excess water was removed, the wet weight recorded (*Wf*) and the final swelling ratio (*SWr*, expressed as a percentage) was calculated according to the formula:

$$SWr = \frac{Wf - W0}{W0} \times 100.$$

2.2.2 Collagen incorporation

The final collagen content of the different groups (A, B, C, D) of Alg-Coll scaffolds was determined from measuring the hydroxyproline content of digested samples (see section 2.8) (n = 3). Constructs were evaluated by Scanning Electron Microscope (SEM, see section 2.9) and through histological staining (Picro Sirius Red for collagen staining, see section 2.10) to ascertain the homogeneity of collagen distribution and to evaluate the micro-structure and porosity.

2.2.3 Assessment of biomechanical properties

Constructs from groups A and C (5mm Ø x 3mm H, n =3) were mechanically tested under confined compression conditions in phosphate buffed saline (PBS) at room temperature using a standard materials testing machine with a 5N load cell (Zwick Z005, Roell, Germany). A preload of 0.01N was applied to ensure that the top surface of the construct was in direct contact with the porous indenter. Stress relaxation tests were performed, consisting of a ramp and hold cycle with a ramp displacement of 1µm/s until 10% strain was obtained (the maximal stress recorded corresponding to the peak stress) and maintained until equilibrium was reached for at least 45 min. (corresponding to the equilibrium stress). The equilibrium modulus was calculated by taking the stress determined at complete relaxation (equilibrium) and dividing by the applied strain (10%) respectively.

2.2.4 Incorporation of TGF-β3 and determination of release profile from alginate-based scaffolds

The influence of collagen incorporation on TGF-β3 release profile from alginate-based scaffolds (5 mm Ø x 3 mm H, n = 3) was evaluated using an Enzyme Linked Immunosorbent

Assay (ELISA). Briefly, scaffolds (Group A, alginate only compared to Group C, alginate-collagen scaffolds) were collapsed with a tweezers and rehydrated with 50 µL of a solution of human transforming growth factor-β3 (TGF-β3, 2.4µg/mL, PeproTech, London, UK). TGF-β3 loaded scaffolds were incubated in 1 mL of PBS at 37°C, and at specific time points (1, 2, 3, 5, 7, 10 and 15 days) the total volume of PBS was removed and replaced with fresh PBS solution and assessed using an ELISA kit according to the manufacturer's instructions (R&D Systems, UK).

2.3 Annulus fibrosus (AF) and bone marrow derived mesenchymal stem cell (MSC) isolation and culture expansion

Porcine annulus fibrosus (AF) and mesenchymal stem cells (MSCs) were harvested from the intervertebral discs (IVDs) and from the bone marrow of the femora respectively (≈ 40 kg / 4 months old) within three hours of sacrifice, as previously described. [16, 25]

Under aseptic conditions, AF tissue was harvested, finely diced and enzymatically digested in 2.5mg/ml pronase solution (Calbiochem, Merck Millipore, Darmstadt, Germany) for 1 hour followed by collagenase digestion at 1mg/mL (Invitrogen, Dublin, Ireland) at 37°C under constant rotation in serum free low-glucose Dulbecco's modified eagles medium (1mg/ml D-Glucose, 200mM L-Glutamine; lg-DMEM) containing antibiotic/antimycotics (100U/ml penicillin, 100µg/ml streptomycin) (all GIBCO, Invitrogen) and amphotericin B (0.25µg/ml, Sigma-Aldrich). Digested tissue/cell suspensions were passed through a 100µm cell strainer to remove tissue debris and washed three times by repeated centrifugation at 650G for 5 min. AF cells were plated at $5x10^3$ cells/cm^2 and expanded in T-175 flasks (Sarstedt, Ireland) in XPAN, corresponding to lg-DMEM supplemented with 10% foetal bovine serum (FBS), penicillin (100U/ml)-streptomycin (100µg/ml) amphotericin B (0.25µg/ml), supplemented

with 5ng/ml Fibroblast Growth Factor-2 (FGF-2; PeproTech, United Kingdom) at 37°C in a humidified atmosphere containing 5% CO_2, with medium changed every 3-4 days.

Mononuclear cells were isolated from the bone marrow and plated at 10×10^6 cells in T-75cm^2 flasks to allow for colony formation. MSCs were maintained in the same XPAN media supplemented with FGF-2 than for the AF cells expansion. Cultures were washed in PBS after 72 hrs. When passaged, MSCs were plated at 5×10^3 cells/cm^2 and expanded to passage 2 in a humidified atmosphere at 37°C and 5% CO_2, with medium changed every 3-4 days.

2.4 *In vitro* annulus fibrosus cell migration study

Agarose moulds were created (agarose type VII, Sigma-Aldrich) with a cavity of 70 µL in the center of each mould (Part A, Fig 4). 50 µL of AF cell suspension at a density of 8.5 x 10^6 cell/mL, similar to the native density of AF tissue, [26] was pipetted into each mould. Alginate only scaffolds (Group A, Alg) and alginate –collagen scaffolds (Group C, Alg-Coll) (3 mm Ø x 3 mm H, n = 3) were collapsed and loaded with either a solution of TGF-β3 (concentration of 2.4µg/mL) or PBS (control). Subsequently, each scaffold was placed into the center of agarose wells and maintained in 24-well plates (Costar Corning, Fisher Scientific, Ireland) with 1mL of XPAN (without FGF-2 supplementation). After 2 days, scaffolds were transferred to fresh 24 well plates with media changed every 3-4 days. Scaffolds were maintained at 37°C in a humidified incubator in low oxygen conditions (5% O_2). Constructs were assessed at days 2, 10 and 21 in terms of cell viability and cytoskeleton fluorescence staining (n=1/2), cell morphology using SEM (n=1/2), DNA content (n=3) and histology (n=2) (n = 6 for each group and each time point).

2.5 Cytocompatibility of MSCs on alginate-based scaffolds

MSCs were seeded onto fully compressed alginate (Group A) and alginate-collagen scaffolds (Group C) (5 mm Ø x 3 mm H). Briefly, MSCs (20 x 10^6 cells/mL) were triturated in a solution of TGF-β3 (concentration of 2.4µg/mL) or in PBS (control). Scaffolds were rehydrated with 50µL of the MSCs/PBS solution or with MSCs/TGF-β3 solution. After seeding, scaffolds were maintained at 37°C in a humidified incubator for 2 hrs to allow for cell attachment and transferred to 24-well plates with 2mL of XPAN with and without TGF-β3 (10ng/ml) supplementation (n = 6 per group). Media was changed twice weekly during the 21 days culture period of the experiment. After 21 days constructs were assessed in terms of cell viability (n = 1), biochemical content (n = 3) and histology (n = 2).

2.6 *Ex vivo* organ culture model

2.6.1 Preparation of full IVDs from bovine coccygeal for *ex vivo* organ culture

IVDs were harvested aseptically from bovine tails as previously described. [27] Briefly, bovine tails (18 months old) were obtained from an abattoir within 3 to 5 hours of sacrifice. As illustrated in figure 1, bovine tails were first cleaned with a solution of iodinated povidone (1:100) for 15 minutes (Videne Antiseptic Solution, Ecolab Ltd, Garforth, UK) and, under sterile conditions, tissues (muscles and tendons) were removed to expose the vertebral endplates of the IVDs (Step 1). Using a custom-made blade-holder, intact IVDs including the cartilaginous endplates were cut, thoroughly cleaned using a jet lavage system (Stryker® Interpulse Irrigation System, Stryker, UK) (in order to enhance the nutrient diffusion through the endplates) and maintained hydrated in sterile gauze soaked with PBS containing penicillin (100U/ml)-streptomycin (100µg/ml) and amphotericin B (0.25µg/ml) (Step 2). Defects in the annulus fibrosus tissue were created using a biopsy punch (Ø 4 mm, 4 defects per IVD) and, subsequently, one scaffold (Ø 5 mm x 4 mm H) was collapsed and inserted into a custom-made catheter of ~ 1 mm diameter, injected into the defect site and rehydrated to completely

fill the volume of the defect (Step 3). IVDs (n = 5) were cultured for 5 weeks in 100 mL of XPAN under gentle agitation (orbital platform shaker, PSU-10i, Biosan, Latvia) at 37°C in normoxic conditions (Step 4), with medium changed twice weekly. Viability of AF cells over the period of culture was evaluated (days 1, 21 and 35) on control IVD (n = 1) using LIVE/DEAD® staining on biopsied AF tissues.

2.6.2 Cell migration study on alginate-based scaffold on *ex vivo* model

The first *ex vivo* experiment aimed to investigate the ability of alginate-based scaffolds to facilitate recruitment of AF cells through migration from the tissue surrounding the defects. Alg (Group A) and Alg-Coll (Group C) scaffolds (5 mm Ø x 3 mm H, n = 4 per group) were prepared as previously described, collapsed and injected into the defect site (4 mm Ø x ~4 mm deep). A solution of growth factor (50µL of TGF-β3 at 2.4µg/mL) was injected into the defect, fully rehydrating the scaffold and allowing it to expand to fill the defect. The IVDs containing "TGF-β3 loaded Alg" and "TGF-β3 loaded Alg-Coll" scaffolds (n = 1 IVD per group and 4 scaffolds per IVD), were maintained in XPAN for 5 weeks. At the end of the culture period, scaffolds were carefully removed and assessed in terms of cell viability (n = 1), histology (n = 2) and SEM (n = 1).

The second *ex vivo* experiment evaluated the potential to deliver MSCs directly into the scaffold after its placement and to investigate - (i) the survival of the MSCs post-implantation, and - (ii) if the presence of MSCs promoted resident AF cell recruitment. In order to monitor the fate of the injected cells, MSCs were first labeled using red fluorescent cell membrane labeling PKH26 according to the manufacturer's instructions (Sigma-Aldrich). The protocol for this experiment is similar to the previously described study on acellular scaffolds, except that the rehydration of implanted scaffolds was achieved with a solution of 50µL containing

the growth factor TGF-β3 (2.4µg/mL) combined with fluorescently labeled-MSCs (20 x 10^6 cells/mL). The IVDs containing "MSC-laden TGF-β3 loaded Alg" and "MSC-laden TGF-β3 loaded Alg-Coll" scaffolds (n = 1 IVD per group and 4 scaffolds per IVD), were maintained in XPAN for 5 weeks. At the end of the organ culture experiment, scaffolds were carefully removed and assessed as previously described.

2.7 Fluorescent cell staining and labelling

2.7.1 Cell viability

Cell viability was assessed using a LIVE/DEAD® viability/cytotoxicity assay kit (Invitrogen, Bio-science, Ireland). Briefly, constructs were cut in half, washed in PBS followed by incubation in PBS containing 2µM calcein AM (green fluorescence for live cells) and 4µM ethidium homodimer-1 (red fluorescence for dead cells; both from Cambridge Bioscience, UK). Sections of constructs were washed in PBS, imaged at magnifications x10 and x20 with an Olympus FV-1000 Point-Scanning Confocal Microscope (Southend-on-Sea, UK) and analyzed using FV10-ASW 2.0 Viewer software.

Due to the spectro-incompatibility between the fluorescence emitted from the ethidium and that of PKH26, for experiments using PKH26-labelled MSCs, ethidium was replaced by another DNA-binding probe, DRAQ7™ (Biostatut Limited, Leicestershire, UK) to stain non-viable cells (dilution of 1:100). Due to the low number of samples per group (n=1) only qualitative results of the live and dead cells are presented.

2.7.2 Actin cytoskeleton staining

Scaffold cross-sections were incubated with fluorescent rhodamine-conjugated phalloidin (dilution 1:40, Biotium, Hayward, USA) combined with Hoechst (DAPI, dilution 1:50, VWR,

Ireland) in order to identify cell morphology and observe F-actin filaments of the cytoskeleton (in red) and the nucleus of the cell (in blue).

2.8 Quantitative biochemical analysis

To quantify the accumulation of biochemical constituents, constructs were digested with 125μg/mL papain in 0.1M sodium acetate, 5mM L-cysteine-HCl, 0.05M EDTA, pH 6.0 (all from Sigma-Aldrich) at 60°C under constant rotation for 18 hrs (n=3 for each group). DNA content of each sample was quantified using the Hoechst Bisbenzimide 33258 dye assay, with a calf thymus DNA standard. Total collagen content was estimated by measuring the hydroxyproline content using trans-4-Hydroxy-L-proline standard stock solution at 1 mg/mL (Fluka, Ireland). Samples were hydrolyzed at 110°C for 18 hrs in 38% HCl and assayed using a chloramine-T assay. [28]

2.9 Scanning Electron Microscope (SEM) examination

Prior to Scanning Electron Microscope (SEM) observation, scaffolds were cut in half and fixed with 4% paraformaldehyde solution (PFA) in sodium cacodylate – barium chloride buffer at 4ºC overnight followed by repeated washings in PBS. Fixed samples were dehydrated through successive graded ethanol baths (10 to 100%) followed by critical point drying with CO_2. Scaffolds were then sputter coated with an approximate 10nm thick gold film, and examined by SEM (Tescan Mira FEG-SEM XMU, Libušina, Czech Republic) using a lens detector with a 5kV acceleration voltage at calibrated magnifications.

2.10 Histology and immunohistochemistry

Staining of matrix deposition in the scaffolds was performed after fixation, dehydration and wax embedding. Briefly, constructs were removed from the culture media, washed in PBS

and fixed in 4% PFA solution in sodium cacodylate – barium chloride buffer overnight at 4ºC. After removing the fixative and washing, samples were gradually dehydrated through 70-100% ethanol series with a final xylene change, before embedding in wax. Sections of 8µm were obtained with a microtome (Leica RM2125RT, Ashbourne, Ireland) and affixed to microscope slides (Polylysine^{TM}, VWR, Dublin, Ireland). Prior to staining, sections were dewaxed and rehydrated in 100-70% ethanol baths followed by distilled water. Cellular colonization and matrix deposition was stained using haematoxylin and eosin (H&E), whereas collagen distribution was assessed histologically using Picro-Sirius Red. Cellular infiltration on rehydrated scaffold sections was observed using nuclear fluorescent DAPI staining.

Collagen types I and II were evaluated through immunohistochemistry. Briefly, sections were treated with peroxidase, followed by treatment with chondroitinase ABC (Sigma-Aldrich) in a humidified environment at 37°C to enhance permeability of the extracellular matrix. Sections were incubated with goat serum to block non-specific sites and collagen type I (ab6308, 1:400; 1mg/mL), collagen type II (ab3092, 1:100; 1mg/mL) primary antibodies (mouse monoclonal, Abcam, Cambridge, UK) were applied for 18 hrs at 4ºC. Next, the secondary antibody (Anti-Mouse IgG biotin conjugate, 1:200; 2.1mg/mL) (Sigma-Aldrich) was added for 1 hr followed by incubation with ABC reagent (Vectastain PK-400, Vector Labs, Peterborough, UK) for 45 min. Colour was developed using the Vectastain ABC reagent followed by exposure to peroxidase DAB substrate kit. Negative and positive controls of porcine ligament and cartilage were included for each batch.

2.11 Statistical analysis

Statistical analyses were performed using GraphPad Prism (version 5) software with 3 samples analyzed for each experimental group. One way ANOVA was used for analysis of

variance with Bonferroni's post-tests to compare between groups. Results are reported as mean ± standard deviation. Significance was accepted at a level of $p < 0.05$.

3 Results

3.1 Physical characterisation of alginate and alginate-collagen scaffolds

Alginate-collagen scaffolds were successfully fabricated with specific amounts of collagen as determined through biochemical analyses (Fig. 2A). The intrinsic shape-memory property of covalently crosslinked alginate was not affected with the incorporation of collagen, with all scaffolds (Groups A-D) exhibiting similar swelling ratios (Figs 2B). The average weight of the scaffolds (5 mm Ø x 3 mm H) before rehydration was 1.12 +/- 0.12 mg and after rehydration and swelling was 35.93 +/- 4.36 mg (data not shown), which globally corresponds to swelling ratios ranging between 3000 to 4000%, independent of the collagen incorporation. Up to 7% of collagen could be successfully incorporated into the scaffold (expressed as a percentage compared to alginate dry weight) using a concentration of collagen solution at 2.26 mg/mL. In this study, we observed that the incorporation of collagen into the alginate porous scaffold did not significantly alter the mechanical properties of the composite scaffold compared to alginate only, in terms of peaks stress and equilibrium modulus (Fig. 2C). Higher concentrations (i.e. 4.52 mg/mL) did not enhance the final amount of collagen into the scaffold due to the increased solution viscosity and difficulties with infiltration. Alginate scaffolds containing 7% collagen retained their initial geometry after rehydration with PBS within 5 sec. (Fig. 2D, Supplementary Video S.1 and SD1 (A-C)). Interestingly, this scaffold exhibits excellent elastic properties, as it is able to quickly recover its original shape after compression (SD1 D-F). Collagen coating deposition onto the alginate struts was confirmed by microscopic analyses (i.e. using scanning electron microscope, SEM) (Figs 3A-D). We observed that with low concentrations of collagen (i.e. 1.13 and 2.26 mg/mL), collagen fibers

were homogenously distributed into the alginate porous structure (Figs 3B and C). In contrast, for higher collagen concentration, deposition of collagen was confined to the outer part of the scaffold (Fig. 3D), possibly due to viscosity effects. Appreciation of collagen distribution within the alginate scaffolds using histological technique (i.e. Picro Sirius Red) did not permit discrimination due to background staining of the alginate itself (Figs 3E-H). However, from SEM observations, we noted that for a collagen concentration of 4.52 mg/mL, a dense layer of collagen was formed around the periphery of the scaffold. Consequently, for all subsequent *in vitro* culture experiments we selected Group C Alg-Coll scaffold (2.26 mg/ml), with the Alg scaffold (Group A) serving as a control.

3.2 AF cell migration in alginate-based scaffolds

3.2.1 *In vitro* assessment

The addition of collagen into alginate scaffolds had a considerable effect on AF cell migration (Fig. 4). By day 2, DNA quantification of Alg (Group A) and Alg-Coll scaffolds (Group C) revealed that the incorporation of collagen into the alginate scaffold significantly enhanced cellular attachment to the scaffold (Fig. 4A). Few cells were observed to adhere to alginate only scaffolds (Alg) compared to Alg-Coll scaffolds in which a higher proportion of cells were present in the peripheral regions of these scaffolds (Figs 4B and D). Interestingly, at days 10 and 21, cells did not proliferate as the total amount of DNA for each group was similar ($p>0.05$) (Fig. 4A). Histological analyses revealed that for control scaffolds (Alg), cells did not colonize the scaffold but remained in smalls cluster during the 3 weeks of the *in vitro* experiment (Fig. 4C). In contrast for Alg-Coll scaffolds cells migrated and colonized the entire volume (Fig. 4E).

Minor differences between TGF-β3 loaded and non-loaded scaffolds was observed for both Alg only and Alg-Coll groups. In order to investigate this moderate bioactivity of the TGF-β3

loaded scaffold, we examined the release kinetics of TGF-β3 growth factor using an ELISA. The release kinetics of TGF-β3 from both Alg and composite Alg-Coll scaffolds was rapid with almost 98% released within the initial 24 hrs (SD.2), which could possibly explain the limited bioactivity on AF cells.

Additional *in vitro* experiments revealed that both scaffold types were capable of supporting cell viability (Fig. 5). However there were distinct differences in cell shape depending on scaffold type. Specifically, by day 21 for Alg scaffolds, AF cells remained viable (Fig. 5A) but H&E staining showed that cells did not migrate and colonize the scaffold structure (Fig. 5B). Instead small clusters of cells were observed (Figs 5C and D). Furthermore, the limited presence of F-actin in the cytoskeleton demonstrates that the cells were not able to readily attach to the alginate scaffold material (Fig. 5E). In comparison, for Alg–Coll scaffolds, after 21 days, AF cells exhibited excellent viability (Fig. 5F) and have migrated and penetrated into the volume of the scaffold (Figs 5G and H) with no cell clustering observed. Indeed, AF cells exhibited a pronounced spindle-shape morphology (Fig. 5I) and cytoskeleton stained intensively positive for F-actin protein (Fig. 5J).

3.2.2 *Ex vivo* organ culture assessment

Scaffolds implanted into the defects remained *in situ* and intact for the entire duration of 5 weeks (Fig. 6A). LIVE/DEAD™ assay on control IVD tissue showed that the viability of AF cells was maintained for the first 21 days with more pronounced cell death observed by day 35 (SD.3). *Ex vivo* studies revealed similar trends and observations as those observed from *in vitro* experiments.

For Alg only scaffolds LIVE/DEAD™ revealed limited migration and infiltration of resident AF cells from the surrounding AF tissue after 5 weeks of implantation (Figs 6B and C). This was also confirmed through SEM analyses (Fig. 6D). In comparison, Alg-Coll scaffolds

appeared to stimulate cell recruitment from the peri-implant area, followed by attachment and migration into the scaffold. Indeed, on some external regions of the scaffolds which were in close contact with the native AF tissue, cells attached to the scaffolds creating a migratory front, with subsequent invasion into the porous network of composite constructs with high cell viability being maintained (Figs 6E - G). Histological analyses revealed that limited neo-ECM deposition was secreted by the infiltrated AF cells for both Alg and Alg-Coll constructs (data not shown).

3.3 *In vitro* cytocompatibility of MSCs on alginate-based scaffolds

Having demonstrated that the incorporation of collagen into alginate structures offered significant advantages in terms of AF cell adhesion and scaffold colonization for both *in vitro* and *ex vivo* conditions, we next explored the use of these scaffolds in combination with MSCs. We hypothesized that by loading MSCs into the scaffold during implantation, matrix deposition could be enhanced. Evaluation in IVD-like microenvironmental conditions revealed that MSCs remained viable in both Alg and Alg-Coll scaffolds (unloaded, loaded with TGF-β3 or cultured in TGF-β3 supplemented media). By day 21, DNA quantification for the different scaffolds demonstrated higher cell numbers for Alg-Coll scaffolds compared to alginate only (> 5 fold, Fig. 7A). Collagen content, which is a key constituent of the native AF extracellular matrix was determined using a hydroxyproline assay. Limited deposition of collagen was observed for Alg only scaffolds (in the presence or absence of TGF-β3 loaded in the scaffold or supplemented in the media, data not shown). In comparison, incorporation of collagen into the alginate-based scaffolds positively influenced matrix deposition by MSCs with the presence of TGF-β3 further enhancing matrix deposition (Fig.7B). Indeed, the amount of collagen quantified in constructs cultured in TGF-β3 supplemented media (XPAN + TGF-β3) was 1.95 fold higher compared to unsupplemented media (XPAN) (with values

corresponding to 26.5 µg and 13.6 µg/scaffod respectively). Interestingly, the incorporation of TGF-β3 into Alg–Coll scaffolds appeared to stimulate collagen synthesis compared to cultivation in XPAN only (corresponding to 1.56 fold higher).

For MSCs seeded onto Alg scaffolds, macroscopic imaging revealed limited colonization (Fig.7C), similar to that previously observed for AF cells. LIVE/DEAD® staining showed good cell viability, with cells exhibiting a rounded morphology (Fig. 7D). Histological staining using Picro Sirius Red confirmed the limited collagen deposition in alginate scaffolds (Figs 7E and F). In comparison, for Alg-Coll scaffolds, higher cell activity was observed macroscopically, as the scaffolds were more opaque at the end of the culture period compared to alginate only (Fig. 7G). MSCs exhibited a fibroblastic-like morphology with intense cytoplasmic spreading (Fig. 7H). Histological examination revealed positive collagen staining within the porous network of the constructs (Figs 7I and J). Immunochemistry revealed collagen type I was deposited within the newly formed matrix (Figs 7K and L), whereas no collagen type II was detected (data not shown).

3.4 Cell colonization of MSC-laden alginate-based scaffold in an organ culture model

Having demonstrated that the addition of collagen to the alginate scaffold stimulated MSCs to attach and to proliferate, and that the loading of TGF-ß3 further enhanced matrix deposition; we next explored how this system would perform in an *ex vivo* organ culture model. For the different groups (Alg (Fig. 8 A) and Alg-Coll (Fig.8F)), the implanted scaffolds remained in the defect site of the IVD for the 5 weeks of the experiment, with no variation in terms of volume or size observed. Control group, corresponding to MSCs injected in TGF-β3 loaded Alg scaffold, demonstrated limited cell proliferation into the scaffold after 5 weeks of culture but instead created small clusters, similar to that observed from *in vitro* experiments. The

LIVE/DEAD™ assay demonstrated that the cells were mainly viable (Figs 8B and C) and that the clusters of cells were composed almost exclusively of MSC-labeled cells (Fig.8D) (as the proportion of red-stained MSC-labeled cells was globally similar to the total cell population). The ability of native AF cells to migrate from the tissue surrounding defect site was limited (as previously demonstrated *in vitro*, Fig.6) even with the presence of MSCs.

In comparison, in Alg-Coll constructs, a higher number of cells were able to proliferate throughout the scaffold, and cells remained viable during the 5 weeks of the study (Figs 8G and H). Compared to Alg only, Alg-Coll composite scaffolds facilitated migration of AF cells from the surrounding tissue into the scaffold. By day 35, scaffolds were colonized by a heterogeneous cellular population based on MSCs (injected at day 0) and endogenous migrating AF cells (Figs 8G-I). Additionally, SEM analyses confirmed cellular infiltration from the outer part of the Alg-Coll scaffold (Fig. 8J).

4 Discussion

Tissue engineering strategies for annulus fibrosus regeneration of the intervertebral disc is still in its infancy. [8, 9, 29] We have previously demonstrated that porous scaffolds based on covalently crosslinked alginate using carbodiimide chemistry is an attractive biomaterial for tissue repair. [16] Due to the chemical modification of the alginate chains, the resulting structure is more stable than alginate hydrogels typically obtained through ionic crosslinking, and more importantly, exhibits shape-memory properties upon hydration. Such physical characteristics are highly attractive to regenerate damaged tissues and offer the potential for minimal invasive surgery via injection with the ability to expand and fill defects of various shapes, geometries and sizes. However, to foster regeneration, such scaffolds should facilitate cell attachment, migration and colonization of the porous construct shortly after its insertion into the host tissue.

We have previously shown that AF cells isolated from porcine IVD have the capacity to proliferate in alginate scaffolds and to secrete a large amount of extracellular matrix in IVD-like microenvironmental condition in the presence of TFG-β3. [16] However, we observed that cells did not attach directly on the hydrophilic surface of the scaffold, which has also been reported by other authors. [30, 31] Indeed, structures fabricated from highly hydrophilic polymers do not lend themselves to protein adsorption and are therefore poor substrates for cellular adhesion. [11, 30] This characteristic has been largely observed *in vitro* for osteoblasts, [32, 33] skeletal myoblasts, [34] chondrocytes, [35, 36] hepatocytes [37] and nucleus pulposus cells, [38, 39] where cells exhibited weak adhesion and proliferation after encapsulation in unmodified alginate.

Biomimetic based scaffolds based on collagen have been investigated as potential candidates to regenerate the AF tissue [40, 41] since collagen is a major biological constituent of the AF matrix (50-70% dry weight). [42] In addition, collagen exhibits several advantages in terms of immunogenicity and biocompatibility. [8] However, collagen-based constructs are inherently weak mechanically and are susceptible to shrinkage when cultured with cells limiting their applicability for tissue repair. Indeed, the reduction in volume of 3D collagen scaffolds after 35 days of *in vitro* cultivation has previously been reported to be up to ninefold [43] with concomitant loss in mass after only 14 days. [44, 45]

We have previously demonstrated that alginate only scaffolds did not support cell attachment. [16] In the current study, in an attempt to enhance the ability of cells to adhere and to colonize the scaffold, we investigated the incorporation of collagen as a biological matrix into freeze-dried alginate porous constructs to overcome such limitations.

This collagen-enriched alginate scaffold exhibited similar physical properties to alginate only scaffold in terms of swelling, compressive and shape-memory behavior, added to the fact that scaffolds retained their initial size and shape during throughout experiments.

Of interest from this work is the significant influence that collagen had in regulating cell behavior, in terms of cell shape/ morphology and migration. Preservation of AF cell phenotype during *in vitro* cultivation remains challenging as previous studies showed a tendency of the cells to differentiate towards an NP-like phenotype with overexpression of collagen type II and aggrecan genes. [46, 47] A major prerequisite for any cell-based therapies aiming to recreate biologically functional AF tissue is to be able to deliver the cells in an appropriate vehicle which maintains the correct cell phenotype. [48]

In alginate only, AF cells exhibited a rounded shape morphology, closer to the chondrocyte-like phenotype of nucleus pulposus cells; whereas in collagen-enriched scaffolds, cells attached and exhibited an elongated fibroblastic-like phenotype, typical of AF-cells morphology. [49]

Ex vivo organ culture experiments are highly attractive as they more closely mimic the *in vivo* scenario, offering a more challenging environment than *in vitro* conditions. Discs isolated from the bovine coccygeal have been proposed as a suitable alternative to human IVD, in terms of ECM distribution, [50, 51] swelling pressure [52] and size [53] compared to other animal species and is easily accessible. *Ex vivo* organ culture experiments showed that TGF-ß3 loaded Alg-Coll scaffolds significantly promoted recruitment of endogenous AF cells from the surrounding surgical defect area and infiltration into the 3D constructs compared to Alg only. However, in contrast to the *in vitro* migration studies which demonstrated rapid cellular colonization of Alg-Coll scaffolds, *ex vivo* organ culture studies on these acellular scaffolds revealed that the colonization by endogenous AF cells from the injured IVD is not rapid which may pose an issue for implant integration with host tissue.

As a consequence, cell-based approaches to promote IVD therapy have been proposed using transplanted autologous cultured disc-derived chondrocytes (ADCT) [54] or mesenchymal stem cells. [44, 55-59] See et al. demonstrated the potential of differentiating MSCs towards an inner-

AF cell phenotype. [60, 61] Such strategies offer tremendous advantages compared to autologous AF cell transplantation in terms of availability, ease of harvesting, tissue morbidity, pain and subsequent risk of disc herniation for the donor. In this study, we showed that, *in vitro*, under IVD-like microenvironmental conditions, collagen-alginate scaffolds were capable of maintaining MSC viability and facilitated matrix accumulation. Moreover, accumulation of collagen into the scaffold (collagen type I) was stimulated by the intrinsic delivery of growth factor (TGF-β3) compared to TGF-β3 free media. Organ culture experiments containing scaffolds seeded with MSCs facilitated the retention and sustained the survival of transplanted MSCs for at least 5 weeks.

This is a primary prerequisite for cell-based therapy as the risk of cell leakage and poor cell survival post injection into the center of the IVD has been well documented in *ex vivo* experiments. [62] Microscopic analyzes performed on scaffolds at the end of the culture study revealed the presence of a heterogeneous cellular population, consisting of a mixture of MSCs and endogenous AF cell population from the donor site. However, histological evaluation of excised constructs revealed limited tissue ingrowth within the porous constructs. From this preliminary work, we showed that delivering a scaffold seeded with MSCs to a damaged area of the IVD offers limited benefit in terms of tissue regeneration. A number of aspects may need to be optimized in order to elicit a beneficial response such as better control of growth factor release kinetics, increasing the seeding density of MSCs and possibly pre-differentiation of MSCs prior to transplantation.

In our study, we did not observe differences in terms of AF cell migration and MSC proliferation with TGF-ß3 loaded scaffolds compared to unloaded scaffolds, which could clearly restrict the biological activity of this bioactive scaffold system. There are a number of aspects that could be explored or optimized to improve the release kinetics of growth factors by covalently crosslinking to the scaffold. [63] This strategy may prolong the retention of the

active cues in the scaffold environment, and has been successfully applied for many biomedical applications including bone [64] and cartilage. [65]

However, short-term TGF-ß3 exposure in loaded scaffolds did positively influence subsequent collagen deposition by MSCs. This is consistent with the work by Huang et al. showed that continuous TGF-ß3 supplementation did not enhance MSC proliferation, but actually increased GAG and collagen accumulation. [66]

Another limitation of these scaffold materials is the mechanical properties, which are significantly lower than native annulus fibrosus tissue. [16] Nevertheless, the function and biological role of such injectable porous scaffolds is to fill the tissue defect, to support cell penetration and matrix deposition. Regarding the manipulation of MSCs prior to transplantation, several approaches could be worth exploring. Activation of MSCs towards an AF cell phenotype could be investigated in a co-culture model [67] or by pre-differentiation of pluripotent stem cells prior to transplantation, which has been investigated for articular cartilage regeneration. [68] Seeding cell density is also an important factor that could be investigated, as it directly impacts cell growth and survival, [69] and could consequently increase matrix formation. Nonetheless, the *ex vivo* IVD culture system described in this study provides an attractive model for screening therapeutic systems intended to treat AF defects prior to large animal trials.

However, the authors are conscious of the limitations of such *ex vivo* models. Recent investigations performed on whole IVDs have demonstrated that organs responded to the artificial environment with a degenerative process, [70, 71] which seems to be even exacerbated during the cultivation of IVDs under free-swelling condition. Indeed, mechanical stimuli is known to influence cell phenotype (de)-differentiation, [61] tissue viability, [70] metabolism activity, [72] matrix organization [73] and tissue remodeling [74] on disc cells. In this study, the culturing of IVDs under free-swelling condition during the 5 weeks of the culture period

could explain the poor ECM accumulation observed in the implanted scaffolds. Another important issue to question is how these implanted scaffolds would respond in a loaded mechanical environment. Risk of implant migration and extrusion must be assessed, and sealant materials (i.e. fibrin glue, [75, 76] genipin crosslinking [77] or biodegradable glue [78]) warrant further investigations. However, further investigations will be required to determine if the addition of collagen into the alginate scaffold will elicit a beneficial response *in vivo* in terms of tissue integration, without fibrosis and scar tissue formation, as has previously been observed for collagen based scaffolds. [13]

5 Conclusion

Regeneration of damaged annulus fibrosus tissue using tissue engineering strategies remains a significant challenge. In this work, we demonstrated that collagen can be incorporated into alginate-based shape-memory scaffolds offering advantages over alginate or collagen alone, in terms of mechanical stability, injectability and biological activity; which are highly attractive for the regeneration of AF tissue. *In vitro* studies demonstrated that the addition of collagen into the pre-formed alginate scaffolds promoted annulus fibrosus cell penetration and allow to preserve the natural cell phenotype. In MSC-seeded scaffold, the incorporation of collagen had a tremendous effect on cell proliferation and ECM deposition, and the matrix secretion was even amplified by the local release of TGF-ß3 growth factor compared to non-supplemented media. *Ex vivo* experiments demonstrated that such scaffolds were able to be administered into defects occurring in the AF tissue in a minimally invasive fashion to fill the defect site. Collagen-enriched scaffolds maintained MSC viability and allowed attachment of endogenous AF cells from the surrounding tissue and infiltration into the 3D constructs compared to alginate only scaffolds.

6 Acknowledgments

This work was supported with resources/facilities of the Trinity Centre for Bioengineering and the MSc in Bioengineering programme. The authors would like to thank Dr. Gavin McManus (School of Biochemistry and Immunology, Microscopy and Imaging Facility Trinity Biomedical Sciences Institute) and Neal Leddy (Centre for Microscopy and Analysis, TCD) for their technical assistance.

7 Figure legends

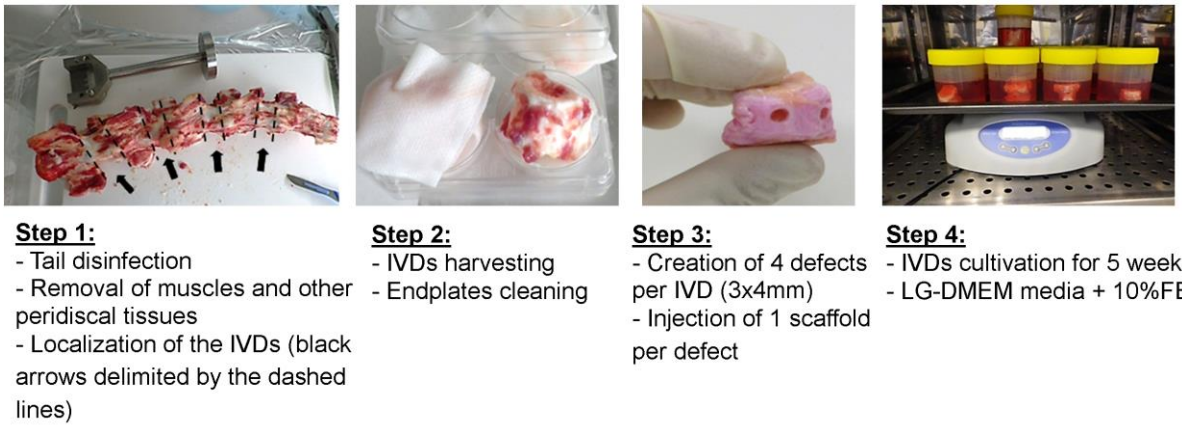

Fig. 1: IVD isolation from bovine coccygeal tissue for *ex vivo* organ culture experiments.

(Step 1) Bovine tails were cleaned and tissues were trimmed to facilitate the localization of the IVDs. **(Step 2)** Using a custom-made blade-holder, intact IVDs were cut, cleaned and maintained hydrated. **(Step 3)** Defects in the AF tissue of each IVD were created using a biopsy punch (Ø 4 mm x 4 mm deep). Using a catheter of ~ 1 mm diameter, one scaffold was injected per defect and rehydrated to completely fill the volume of the defect. **(Step 4)** IVDs were finally cultivated for 5 weeks on an orbital shaker.

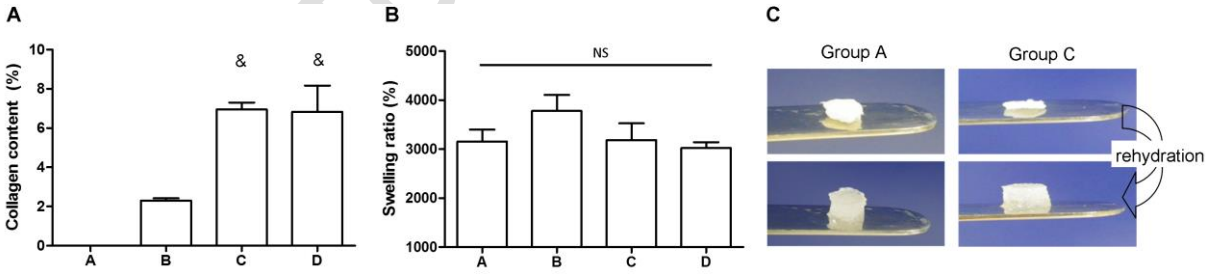

Fig. 2: Physical characterization of alginate and alginate-collagen scaffolds. (A) Quantification of collagen incorporation in alginate-based scaffolds (expressed as a percentage, compared to alginate dry weight) (& indicates significance compared to the alginate-collagen scaffold group B, $p < 0.05$), and **(B)** evaluation of the swelling ratio (%) of alginate and alginate-collagen freeze-dried scaffolds (A = 0 mg/mL, B = 1.13 mg/mL, C = 2.26 mg/mL and D = 4.52 mg/mL). **(C)** Evaluation of the peak stress (kPa) and the

equilibrium modulus (EQM) (kPa). NS indicates no statistical significance between scaffold groups. **(D)** Demonstration of the swelling behavior of alginate scaffolds (Group A) compared to alginate-collagen scaffolds (Group C).

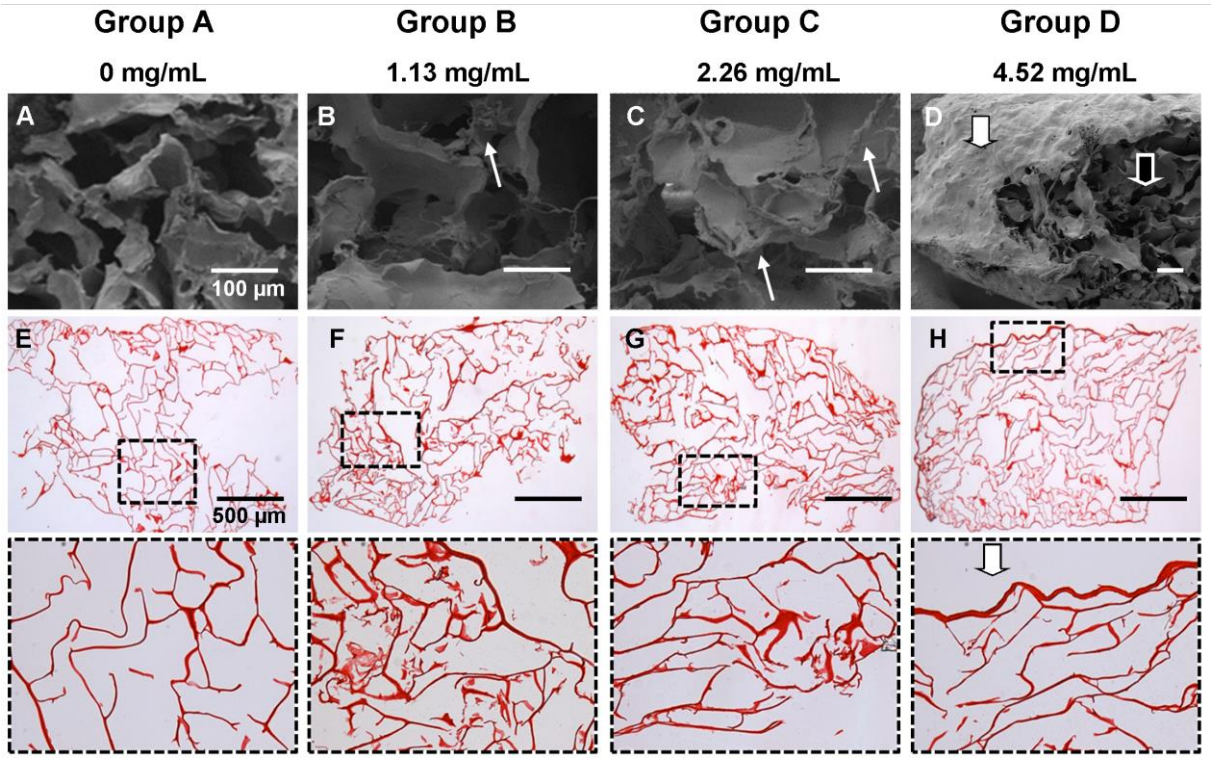

Fig. 3: Microscopic observation of Alg-Coll scaffolds for increasing collagen concentration. (A-D) Scanning Electron Micrographs of collagen deposition and localization (concentrations of 0, 1.13, 2.26 and 4.52 mg/mL for group A, B, C and D respectively).White arrow heads indicate collagen deposition on alginate walls. Large white arrow heads indicate accumulation of collagen layer on the outer periphery of the porous scaffold (alginate wall is indicated by large black arrow head) at the highest collagen concentration (4.52 mg/ml). **(E-H)** Picro Sirius Red staining (magnification x 2) of Alg-Coll scaffolds for increasing collagen concentration.

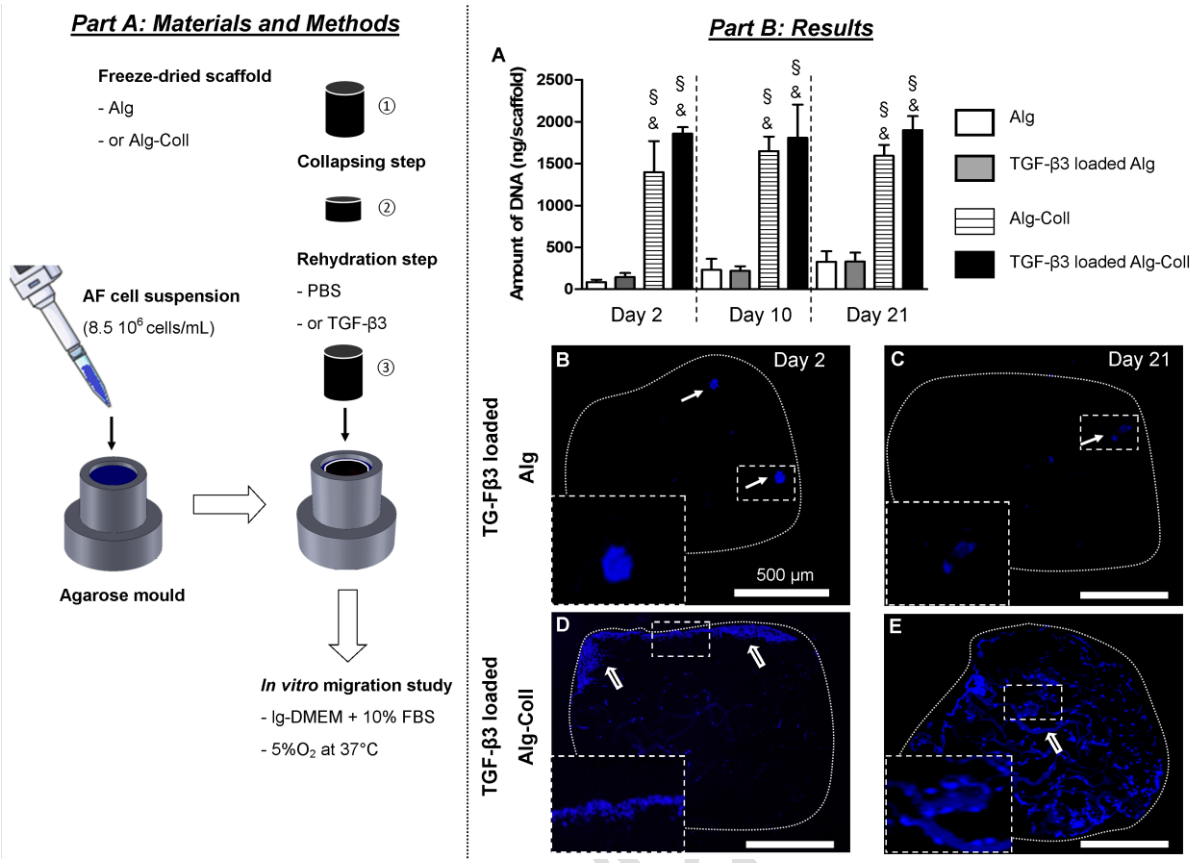

Fig. 4: Evaluation of annulus fibrosus (AF) cell migration in alginate-based scaffolds.

Part A: Schematic presentation of the experimental configuration for the *in vitro* assessment of AF cell migration. Agarose moulds were created and the cavity was filled with AF cell suspension (50µl). Freeze-dried scaffolds (Alg and Alg-Coll) were collapsed and rehydrated with PBS (control) or with TGF-β3 solution. Subsequently, scaffolds were inserted in the well cavity and incubated in low oxygen concentration (5% O_2) in lg-DMEM with 10% FBS (Day 0). At day 2, 10 and 21, were removed for further analysis (n=6 scaffolds per group).

Part B: Results. (A) Determination of DNA content per scaffold for the different groups at day 2, 10 and 21 (& indicates significance compared to the Alg scaffold and § indicates significance compared to TGF-β3 loaded Alg scaffold for each time-point, $p < 0.05$). **(B, C)** DAPI staining (day 2 and day 21) of cross-sections of TGF-β3 loaded Alg with clusters of cells in Alg scaffold highlighted by white arrows and **(D and E)** TGF-β3 loaded Alg-Coll

scaffolds, at different time-points with cell migration in Alg-Coll highlighted by black-and-white large arrows. The periphery of scaffolds is indicated by white-dotted lines (magnification x 4).

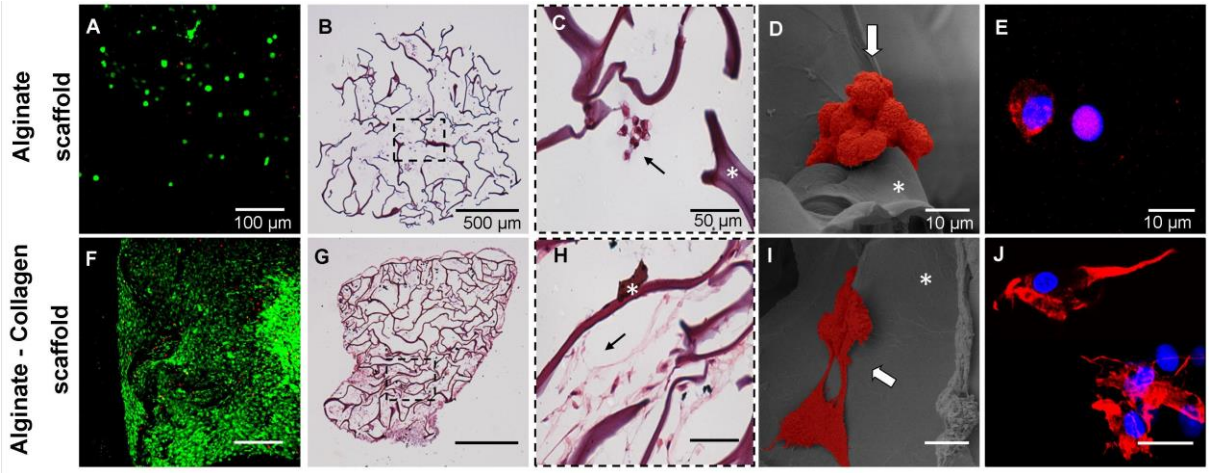

Fig. 5: AF cell behavior is dependent on scaffold type. LIVE/DEAD® staining showing viable cells in green and dead cells in red for **(A)** Alg only compared to **(F)** Alg-Coll scaffold (magnification x 10). **(B and C)** Histological examinations using H&E staining illustrating cluster of AF cells indicated by the black arrow (*indicates the smooth strut material of the alginate scaffold) for Alg only. **(G and H)** spreading of AF cells on Alg-Coll scaffold indicated by the black arrow (magnifications x 4 and x 40 respectively). **(D)** SEM images illustrating agglomeration of AF cells (large white arrow) or **(I)** AF cells spreading (large white arrow) onto the surface of the scaffold (* indicates the alginate wall). To facilitate the distinction between the scaffold and the cells, the cells were artificially colored in red. **(E and J)** DAPI combined with rhodamine fluorescence staining showing the nucleus of the cell in blue and the actin cytoskeletal in red (magnification x 100).

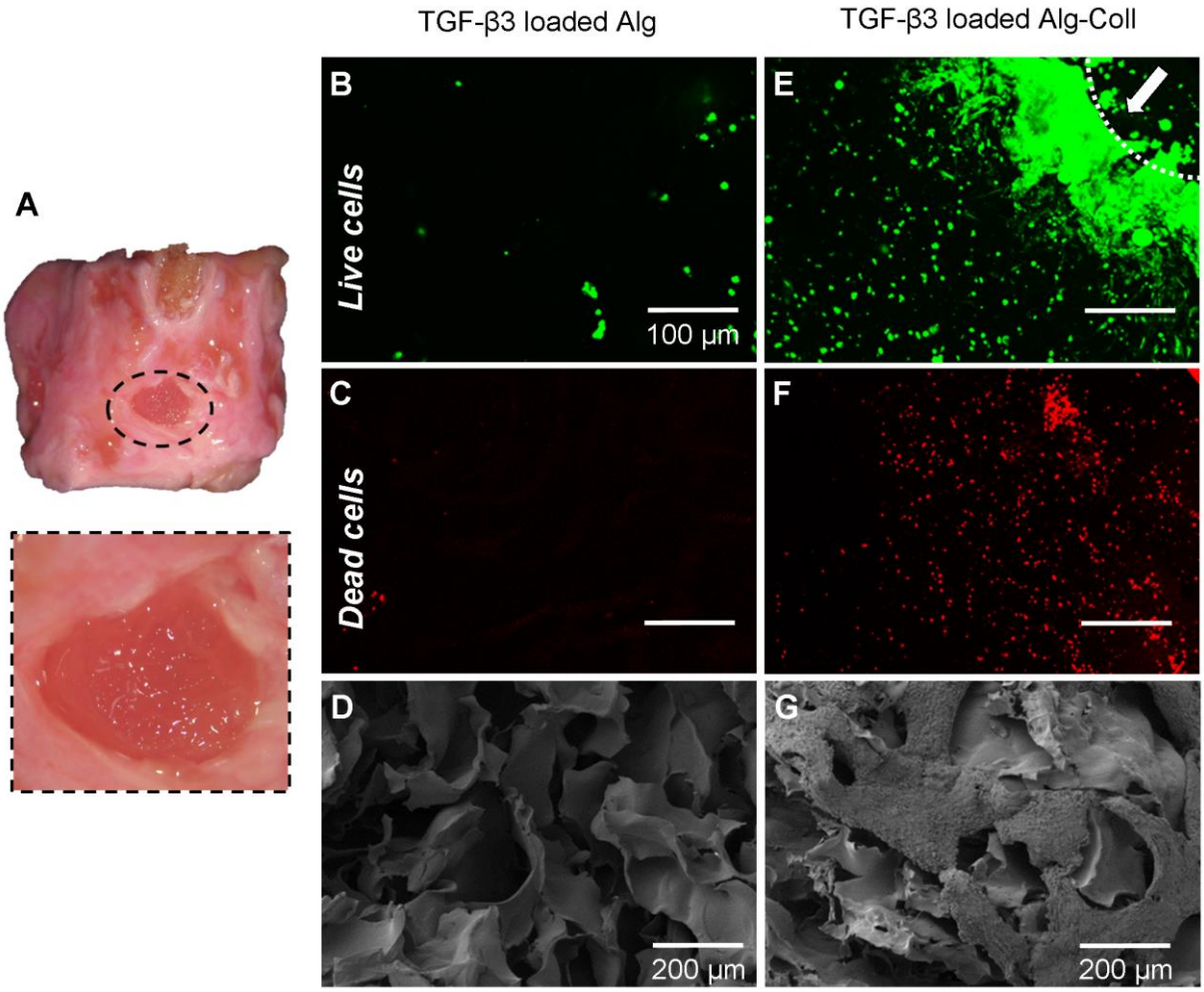

Fig. 6: ***Ex vivo*** **migration study on cell-free TGF-β3 loaded Alg scaffold compared to TGF-β3 loaded Alg-Coll scaffold after 5 weeks of organ culture. (A)** Illustration of the implanted scaffold (TGF-β3 loaded Alg-Coll scaffold) in AF defect of the IVD after 5 weeks of organ culture. **(B and E)** Calcein staining of viable cells (in green) and **(C and F)** ethidium staining of dead cells (in red) for **(B and C)** TGF-β3 loaded Alg compared to **(E and F)** TGF-β3 loaded Alg-Coll scaffold after the 5 weeks of *ex vivo* cultivation (the white dotted line delineates the cell migration front oriented from the peri-implant area of the IVD to the scaffold, magnification x 10). Scanning electron micrographs illustrating **(D)** the absence of cell colonization of the Alg scaffold compared to **(G)** the Alg-Coll scaffold populated by resident AF cells.

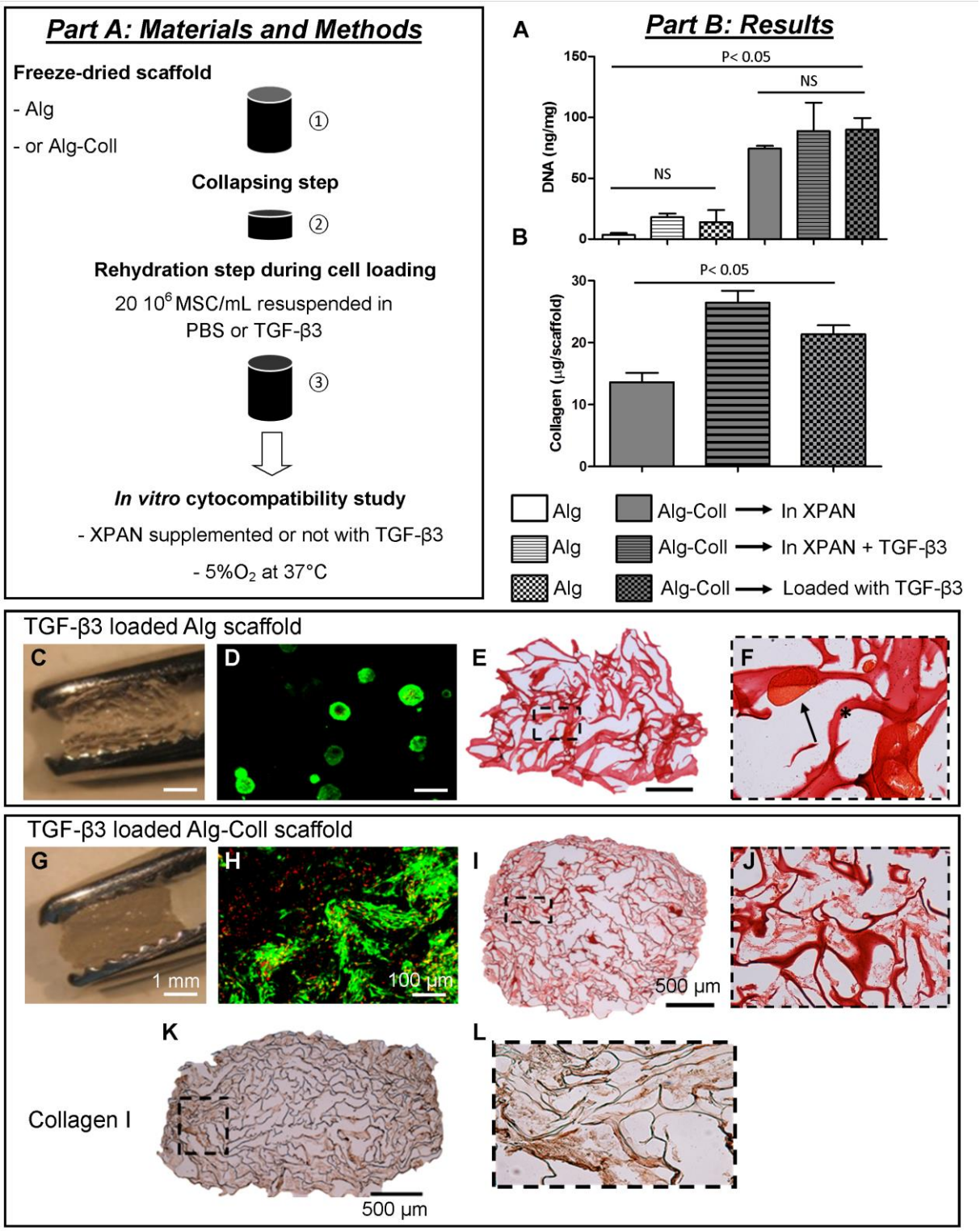

Fig.7: *In vitro* cytocompatibility of MSCs seeded onto Alg and Alg-Coll scaffolds with and without TGF-ß3 incorporation.

Part A: Schematic representation of the *in vitro* cytocompatibility experiment performed on MSC cells on Alg and Alg-Coll scaffolds.

Freeze-dried scaffolds (Alg and Alg-Coll) were collapsed and rehydrated with MSCs suspended in PBS (control) or TGF-β3 solution (2.4µg/mL). Scaffolds were maintained in low glucose and low oxygen (5% O_2) conditions in lg-DMEM with 10% FBS (XPAN) with and without TGF- β3 supplementation for control group or with XPAN only for TGF-β3 loaded scaffolds for three weeks.

Part B: Results. **(A)** DNA quantification for Alg and Alg-Coll scaffolds with and without TGF-β3 loading (no significance was observed for one given scaffold type (Alg or Alg-Coll) depending on the culture condition (with or without TGFβ3 supplementation), but significance was observed between Alg and Alg-Coll scaffolds for each condition, with $P < 0.05$). **(B)** Collagen content of Alg-Coll scaffolds after 21 days of culture in IVD-like environmental condition (low glucose media at 5% O_2), with significance for each condition ($P<0.05$). Collagen content in Alg only scaffolds was below detectable limits (data not presented). **(C-J)** Scaffold appearance, MSC viability and collagen staining in Alg and Alg-Coll scaffolds. **(K and L)** Immunohistochemical staining of Alg-Coll scaffolds for collagen type I. Magnifications: E, I and K = x 4 and F, J, L = x 40.

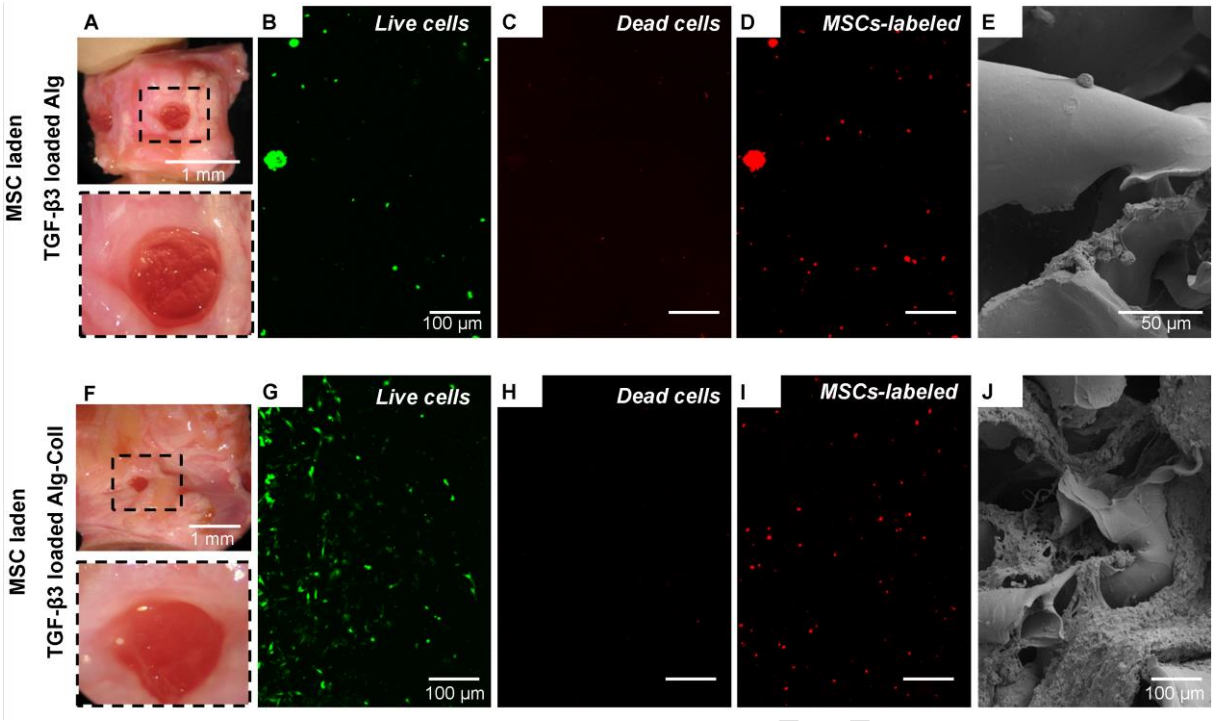

Fig.8: ***Ex vivo*** **study of MSC seeded Alg and Alg-Coll scaffolds loaded with TGF-ß3. (A and F)** Gross macroscopic morphology views of implanted scaffolds after 5 weeks of IVD implantation and illustration of the global cell viability on **(B and C)** Alg compared to **(G and H)** Alg-Coll scaffolds. **(D and I)** Red fluorescent linker PKH-26 allowed localizing the labeled-MSC from the global cell population that colonized the Alg and Alg-Coll scaffold (magnification x 10). Scanning electron microscope observations illustrating **(E)** the limited presence of cells colonization of the Alg scaffold compared to **(J)** the adhesion and scaffold colonization of implanted Alg-Coll constructs by endogenous IVD cells combined with MSC.

8 References

1. Sherman J, Cauthen J, Schoenberg D, et al. Economic impact of improving outcomes of lumbar discectomy. The spine journal. 2010; 10: 108-116.

2. Katz JN. Lumbar disc disorders and low-back pain: socioeconomic factors and consequences. The Journal of bone and joint surgery American volume. 2006; 88 Suppl 2: 21-24.

3. Goubert L, Crombez G and De Bourdeaudhuij I. Low back pain, disability and back pain myths in a community sample: prevalence and interrelationships. European journal of pain. 2004; 8: 385-394.

4. Abdel Shaheed C, Maher CG, Williams KA, et al. Interventions available over the counter and advice for acute low back pain: systematic review and meta-analysis. The journal of pain. 2014; 15: 2-15.

5. Mirza SK, Deyo RA, Heagerty PJ, et al. One-year outcomes of surgical versus nonsurgical treatments for discogenic back pain: a community-based prospective cohort study. The spine journal. 2013; 13: 1421-1433.

6. Whatley BR. Intervertebral disc (IVD): Structure, degeneration, repair and regeneration. Materials Science and Engineering C. 2012; 32: 61-77.

7. Masuda K and Lotz JC. New challenges for intervertebral disc treatment using regenerative medicine. Tissue engineering Part B, Reviews. 2010; 16: 147-158.

8. Guterl CC, See EY, Blanquer SB, et al. Challenges and strategies in the repair of ruptured annulus fibrosus. European cells & materials. 2013; 25: 1-21.

9. Bron JL, Helder MN, Meisel HJ, et al. Repair, regenerative and supportive therapies of the annulus fibrosus: achievements and challenges. European spine journal. 2009; 18: 301-313.

10. Hegewald AA, Medved F, Feng D, et al. Enhancing tissue repair in annulus fibrosus defects of the intervertebral disc: analysis of a bio-integrative annulus implant in an in-vivo ovine model. Journal of tissue engineering and regenerative medicine. 2013.

11. Bidarra SJ, Barrias CC and Granja PL. Injectable alginate hydrogels for cell delivery in tissue engineering. Acta biomaterialia. 2014, 10:1646-1662.

12. Song JE, Kim EY, Ahn WY, et al. The potential of DBP gels containing intervertebral disc cells for annulus fibrosus supplementation:in vivo. Journal of tissue engineering and regenerative medicine. 2013.

13. Grunert P, Borde BH, Hudson KD, et al. Annular Repair Using High-Density Collagen Gel: A Rat-Tail in vivo Model. Spine. 2014; 39: 198-206.

14. Sharifi S, van Kooten TG, Kranenburg HJ, et al. An annulus fibrosus closure device based on a biodegradable shape-memory polymer network. Biomaterials. 2013; 34: 8105-8113.

15. Schek RM, Michalek AJ and Iatridis JC. Genipin-crosslinked fibrin hydrogels as a potential adhesive to augment intervertebral disc annulus repair. European cells & materials. 2011; 21: 373-383.

16. Guillaume O, Daly A, Lennon K, et al. Shape-memory porous alginate scaffolds for regeneration of the annulus fibrosus: effect of TGF-beta3 supplementation and oxygen culture conditions. Acta biomaterialia. 2014; 10: 1985-1995.

17. Chattopadhyay S and Raines RT. Review collagen-based biomaterials for wound healing. Biopolymers. 2014; 101: 821-833.

18. Chevallay B and Herbage D. Collagen-based biomaterials as 3D scaffold for cell cultures: applications for tissue engineering and gene therapy. Medical & biological engineering & computing. 2000; 38: 211-218.

19. Alberts B, Johnson A, Lewis J, et al. Molecular Biology of the Cell. 4th ed. New York: Garland Science, 2002.

20. Ramshaw JAM, Vaughan PR and J.A. W. Applications of collagen in medical devices. Biomed Eng Appl Basis Commun. 2001; 13: 14-26.

21. Tingstrom A, Heldin CH and Rubin K. Regulation of fibroblast-mediated collagen gel contraction by platelet-derived growth factor, interleukin-1 alpha and transforming growth factor-beta 1. Journal of cell science. 1992; 102: 315-322.

22. Tierney CM, Haugh MG, Liedl J, et al. The effects of collagen concentration and crosslink density on the biological, structural and mechanical properties of collagen-GAG scaffolds for bone tissue engineering. Journal of the mechanical behavior of biomedical materials. 2009; 2: 202-209.

23. Haugh MG, Jaasma MJ and O'Brien FJ. The effect of dehydrothermal treatment on the mechanical and structural properties of collagen-GAG scaffolds. Journal of biomedical materials research Part A. 2009; 89: 363-369.

24. Yunoki S, Suzuki T and Takai M. Stabilization of low denaturation temperature collagen from fish by physical cross-linking methods. Journal of bioscience and bioengineering. 2003; 96: 575-577.

25. Thorpe SD, Buckley CT, Vinardell T, et al. The response of bone marrow-derived mesenchymal stem cells to dynamic compression following TGF-beta3 induced chondrogenic differentiation. Annals of biomedical engineering. 2010; 38: 2896-2909.

26. Maroudas A, Stockwell RA, Nachemson A, et al. Factors involved in the nutrition of the human lumbar intervertebral disc: cellularity and diffusion of glucose in vitro. J Anat. 1975; 120: 113-130.

27. Chan SC and Gantenbein-Ritter B. Preparation of intact bovine tail intervertebral discs for organ culture. Journal of visualized experiments. 2012; 60: e3490

28. Kafienah W and Sims TJ. Biochemical methods for the analysis of tissue-engineered cartilage. Methods Mol Biol. 2004; 238: 217-230.

29. Jin L, Shimmer AL and Li X. The challenge and advancement of annulus fibrosus tissue engineering. European spine journal. 2013; 22: 1090-1100.

30. Smetana K, Jr. Cell biology of hydrogels. Biomaterials. 1993; 14: 1046-1050.

31. Lee JH, Khang G, Lee JW, et al. Interaction of Different Types of Cells on Polymer Surfaces with Wettability Gradient. Journal of colloid and interface science. 1998; 205: 323-330.

32. Kuo CK and Ma PX. Ionically crosslinked alginate hydrogels as scaffolds for tissue engineering: part 1. Structure, gelation rate and mechanical properties. Biomaterials. 2001; 22: 511-521.

33. Alsberg E, Anderson KW, Albeiruti A, et al. Cell-interactive alginate hydrogels for bone tissue engineering. Journal of dental research. 2001; 80: 2025-2029.

34. Rowley JA, Madlambayan G and Mooney DJ. Alginate hydrogels as synthetic extracellular matrix materials. Biomaterials. 1999; 20: 45-53.

35. Zeng L, Yao Y, Wang DA, et al. Effect of microcavitary alginate hydrogel with different pore sizes on chondrocyte culture for cartilage tissue engineering. Materials science & engineering C, Materials for biological applications. 2014; 34: 168-175.

36. Mhanna R, Kashap A, Palazzolo G, et al. Chondrocyte Culture in 3D Alginate Sulfate Hydrogels Promotes Proliferation While Maintaining Expression of Chondrogenic Markers. Tissue engineering Part A. 2013.

37. Glicklis R, Shapiro L, Agbaria R, et al. Hepatocyte behavior within three-dimensional porous alginate scaffolds. Biotechnology and Bioengineering. 2000; 67: 344-353.

38. Baer AE, Wang JY, Kraus VB, et al. Collagen gene expression and mechanical properties of intervertebral disc cell-alginate cultures. Journal of orthopaedic research. 2001; 19: 2-10.

39. Chiba K, Andersson GB, Masuda K, et al. Metabolism of the extracellular matrix formed by intervertebral disc cells cultured in alginate. Spine. 1997; 22: 2885-2893.

40. Gruber HE, Leslie K, Ingram J, et al. Cell-based tissue engineering for the intervertebral disc: in vitro studies of human disc cell gene expression and matrix production within selected cell carriers. The spine journal. 2004; 4: 44-55.

41. Saad L and Spector M. Effects of collagen type on the behavior of adult canine annulus fibrosus cells in collagen-glycosaminoglycan scaffolds. Journal of biomedical materials research Part A. 2004; 71: 233-241.

42. Bruehlmann SB, Rattner JB, Matyas JR, et al. Regional variations in the cellular matrix of the annulus fibrosus of the intervertebral disc. J Anat. 2002; 201: 159-171.

43. Bertolo A, Mehr M, Aebli N, et al. Influence of different commercial scaffolds on the in vitro differentiation of human mesenchymal stem cells to nucleus pulposus-like cells. European spine journal. 2012; 21 Suppl 6: S826-838.

44. Sakai D, Mochida J, Iwashina T, et al. Regenerative effects of transplanting mesenchymal stem cells embedded in atelocollagen to the degenerated intervertebral disc. Biomaterials. 2006; 27: 335-345.

45. Sakai D, Mochida J, Iwashina T, et al. Atelocollagen for culture of human nucleus pulposus cells forming nucleus pulposus-like tissue in vitro: influence on the proliferation and proteoglycan production of HNPSV-1 cells. Biomaterials. 2006; 27: 346-353.

46. Chou AI, Reza AT and Nicoll SB. Distinct intervertebral disc cell populations adopt similar phenotypes in three-dimensional culture. Tissue engineering Part A. 2008; 14: 2079-2087.

47. Horner HA, Roberts S, Bielby RC, et al. Cells from different regions of the intervertebral disc: effect of culture system on matrix expression and cell phenotype. Spine. 2002; 27: 1018-1028.

48. Rodrigues-Pinto R, Richardson SM and Hoyland JA. An understanding of intervertebral disc development, maturation and cell phenotype provides clues to direct cell-based tissue regeneration therapies for disc degeneration. European spine journal. 2014.

49. Pattappa G, Li Z, Peroglio M, et al. Diversity of intervertebral disc cells: phenotype and function. J Anat. 2012; 221: 480-496.

50. Roberts S, Menage J, Duance V, et al. 1991 Volvo Award in basic sciences. Collagen types around the cells of the intervertebral disc and cartilage end plate: an immunolocalization study. Spine. 1991; 16: 1030-1038.

51. Demers CN, Antoniou J and Mwale F. Value and limitations of using the bovine tail as a model for the human lumbar spine. Spine. 2004; 29: 2793-2799.

52. Oshima H, Ishihara H, Urban JP, et al. The use of coccygeal discs to study intervertebral disc metabolism. Journal of orthopaedic research. 1993; 11: 332-338.

53. Lee CR, Iatridis JC, Poveda L, et al. In vitro organ culture of the bovine intervertebral disc: effects of vertebral endplate and potential for mechanobiology studies. Spine. 2006; 31: 515-522.

54. Meisel HJ, Siodla V, Ganey T, et al. Clinical experience in cell-based therapeutics: disc chondrocyte transplantation A treatment for degenerated or damaged intervertebral disc. Biomolecular engineering. 2007; 24: 5-21.

55. Chen WH, Liu HY, Lo WC, et al. Intervertebral disc regeneration in an ex vivo culture system using mesenchymal stem cells and platelet-rich plasma. Biomaterials. 2009; 30: 5523-5533.

56. Sobajima S, Vadala G, Shimer A, et al. Feasibility of a stem cell therapy for intervertebral disc degeneration. The spine journal. 2008; 8: 888-896.

57. Leung VY, Chan D and Cheung KM. Regeneration of intervertebral disc by mesenchymal stem cells: potentials, limitations, and future direction. European spine journal. 2006; 15 Suppl 3: S406-413.

58. Sakai D, Mochida J, Iwashina T, et al. Differentiation of mesenchymal stem cells transplanted to a rabbit degenerative disc model: potential and limitations for stem cell therapy in disc regeneration. Spine. 2005; 30: 2379-2387.

59. Orozco L, Soler R, Morera C, et al. Intervertebral disc repair by autologous mesenchymal bone marrow cells: a pilot study. Transplantation. 2011; 92: 822-828.

60. See EY, Toh SL and Goh JC. Simulated intervertebral disc-like assembly using bone marrow-derived mesenchymal stem cell sheets and silk scaffolds for annulus fibrosus regeneration. Journal of tissue engineering and regenerative medicine. 2012; 6: 528-535.

61. See EY, Toh SL and Goh JC. Effects of radial compression on a novel simulated intervertebral disc-like assembly using bone marrow-derived mesenchymal stem cell cell-sheets for annulus fibrosus regeneration. Spine. 2011; 36: 1744-1751.

62. Bertram H, Kroeber M, Wang H, et al. Matrix-assisted cell transfer for intervertebral disc cell therapy. Biochemical and biophysical research communications. 2005; 331: 1185-1192.

63. Hajimiri M, Shahverdi S, Kamalinia G, et al. Growth factor conjugation: Strategies and applications. Journal of biomedical materials research Part A. 2014.

64. Liu HW, Chen CH, Tsai CL, et al. Heterobifunctional poly(ethylene glycol)-tethered bone morphogenetic protein-2-stimulated bone marrow mesenchymal stromal cell differentiation and osteogenesis. Tissue engineering. 2007; 13: 1113-1124.

65. Fan H, Tao H, Wu Y, et al. TGF-beta3 immobilized PLGA-gelatin/chondroitin sulfate/hyaluronic acid hybrid scaffold for cartilage regeneration. Journal of biomedical materials research Part A. 2010; 95: 982-992.

66. Huang AH, Stein A, Tuan RS, et al. Transient exposure to transforming growth factor beta 3 improves the mechanical properties of mesenchymal stem cell-laden cartilage constructs in a density-dependent manner. Tissue engineering Part A. 2009; 15: 3461-3472.

67. Le Visage C, Kim SW, Tateno K, et al. Interaction of human mesenchymal stem cells with disc cells: changes in extracellular matrix biosynthesis. Spine. 2006; 31: 2036-2042.

68. Dashtdar H, Rothan HA, Tay T, et al. A preliminary study comparing the use of allogenic chondrogenic pre-differentiated and undifferentiated mesenchymal stem cells for the repair of full thickness articular cartilage defects in rabbit. Journal of Orthopedic Research. 2011; 29: 1336-1342.

69. Stephan S, Johnson WE and Roberts S. The influence of nutrient supply and cell density on the growth and survival of intervertebral disc cells in 3D culture. European cells & materials. 2011; 22: 97-108.

70. Korecki CL, MacLean JJ and Iatridis JC. Characterization of an in vitro intervertebral disc organ culture system. European spine journal. 2007; 16: 1029-1037.

71. Seol D, Choe H, Ramakrishnan PS, et al. Organ culture stability of the intervertebral disc: rat versus rabbit. Journal of orthopaedic research. 2013; 31: 838-846.

72. Wang C, Gonzales S, Levene H, et al. Energy metabolism of intervertebral disc under mechanical loading. Journal of orthopaedic research. 2013; 31: 1733-1738.

73. Reza AT and Nicoll SB. Hydrostatic pressure differentially regulates outer and inner annulus fibrosus cell matrix production in 3D scaffolds. Annals of biomedical engineering. 2008; 36: 204-213.

74. Chan SC, Ferguson SJ, Wuertz K, et al. Biological response of the intervertebral disc to repetitive short-term cyclic torsion. Spine. 2011; 36: 2021-2030.

75. Buser Z, Kuelling F, Liu J, et al. Biological and biomechanical effects of fibrin injection into porcine intervertebral discs. Spine. 2011; 36: E1201-1209.

76. Colombini A, Ceriani C, Banfi G, et al. Fibrin in Intervertebral Disc Tissue Engineering. Tissue engineering Part B, Reviews. 2014.

77. Likhitpanichkul M, Dreischarf M, Illien-Junger S, et al. Fibrin-genipin adhesive hydrogel for annulus fibrosus repair: performance evaluation with large animal organ culture, in situ biomechanics, and in vivo degradation tests. European cells & materials. 2014; 28: 25-38.

78. Blanquer SB, Sharifi S and Grijpma DW. Development of poly(trimethylene carbonate) network implants for annulus fibrosus tissue engineering. Journal of applied biomaterials & functional materials. 2012; 10: 177-184.